

AEOLIAN BEDFORMS IN THE ESA/ROSCOSMOS EXOMARS 2020 LANDING SITE OF OXIA PLANUM (MARS).

S. Silvestro^{1,2}, D.A. Vaz³, F. Salese^{4,5}, M. Pajola⁶, C.I. Popa¹, G. Franzese¹, G. Mongelluzzo^{1,7}, C. Porto¹, A.C. Ruggeri¹, F. Cozzolino¹ and F. Esposito¹, ¹INAF Osservatorio Astronomico di Capodimonte, Napoli, Italy (simone.silvestro@inaf.it), ²SETI Institute, Mountain View, CA, USA, ³Centre for Earth and Space Research of the University of Coimbra, Coimbra, Portugal, ⁴Faculty of Geosciences, Utrecht University, Utrecht, The Netherlands, ⁵IRSPS, Università Gabriele D'Annunzio, Pescara, Italy, ⁶INAF Osservatorio Astronomico di Padova, Italy, ⁷Department of Industrial Engineering, Università "Federico II", Napoli, Italy

Introduction: The ESA ExoMars rover, Rosalind Franklin [1], will land on Mars on 2021. Water-bearing minerals such as clays and hydrated silica have been detected at Oxia Planum (landing site) suggesting evidence of a wet Mars [2, 3]. The landing ellipse is partially covered by bright aeolian bedforms or Transverse Aeolian Ridges (TARs) showing different morphologies [4, 5, 6]. Here we present results of automatic mapping of TAR locations, wavelengths and orientations, within the landing ellipse (Fig. 1). The morphology of TARs can provide information about the winds regime at the landing site.

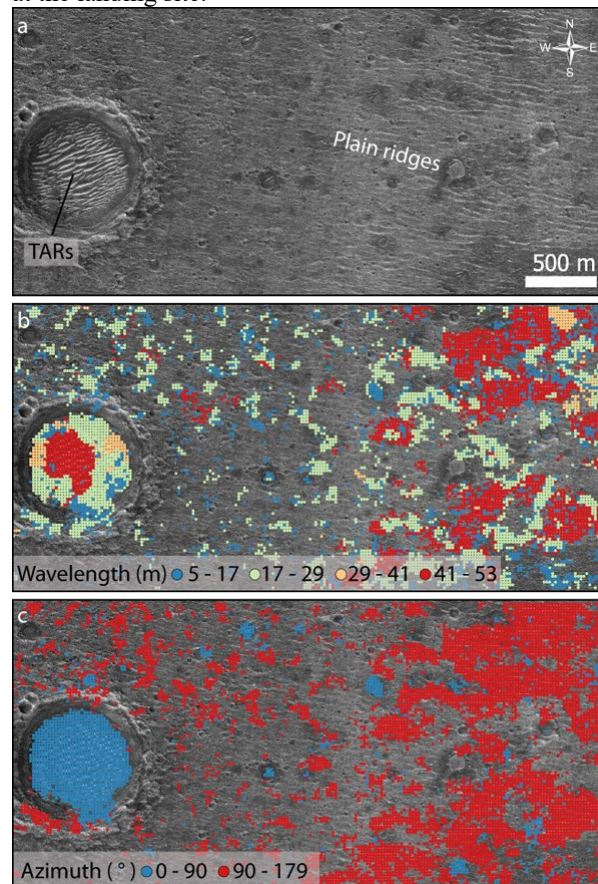


Fig. 1: a) TARs and plain ridges in the landing ellipse showing different wavelength (b) and azimuth (c). Note the different crestline/ridge orientations in panel (c) blue: intra-crater TARs + plain mini-TARs, red: plain ridge pattern.

Methods: TARs parameters were retrieved using HiRISE images [7] acquired along the landing ellipse and coregistered over CTX mosaics [8, 9] in a GIS environment. Wavelength and trend ($0 - 179^\circ$) have been derived automatically and other image texture descriptors were locally computed on the frequency-domain. Supervised neural networks are then used to automatically map the location of aeolian bedforms (Fig. 1).

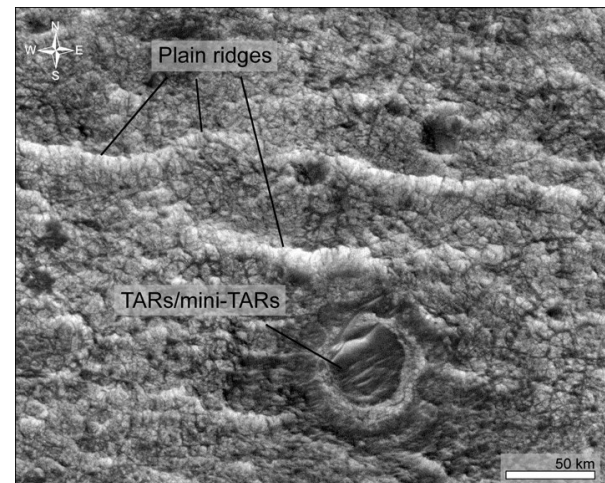


Fig. 2: Mini-TARs and plain ridges on the landing ellipse (HiRISE). Note the Y junction formed by the plain ridges and their eroded and fractured appearance suggesting a PBRs origin.

Results: Previous results of TAR analysis in the landing ellipse highlight the main E-W distribution of the bedform crestlines [6]. In our analysis we show the presence of a set of ENE-WSW oriented TARs within some impact craters and on the surrounding plain [4, 5, 6]. This set of bedforms has wavelength varying from 5 to 53 meters. TARs inside impact craters show exposed cross-beds visible as bright and dark-toned banding over their SE dipping slopes. Similar layers characterize the plain megariipples at NASA MER Opportunity landing site in Meridiani Planum [4, 10]. When identified on the plain, TARs with the same trend have lower height and

wavelength (Fig. 1b). These plain TARs have been previously classified as mini-TARs [4]. The mini-TARs pattern overlies a set of WNW-ESE pattern of ridges (Figs. 1a and 2). These ridges are pervasive on the surrounding plain, they are regularly spaced, cratered and eroded (Fig. 2). Locally Y-junctions can be seen (Fig. 2). These ridges have a variable wavelength with most of them being 41 to 53 meter spaced and they apparently overly the clay-bearing unit [5]. In some cases, bedrock fractures/joints seem to transect the ridges (Fig. 2).

Discussion: The location of the exposed cross-beds over the SE dipping TAR slopes (the TAR stoss side) implies winds blowing from the SE to the NW. Most regional wind indicators, such as sand dunes accumulated in craters nearby the landing ellipse and wind streaks, point to winds coming from a different direction, the NE and NW in good agreement with the mean wind zonal circulation during the Martian southern summer [11]. The different cross-beds albedo on the TARs stoss side might indicate different grains sizes and compositions suggesting bimodal grain size typical of megaripples [12]. The mini-TARs on the plain show a comparable orientation suggesting similar formative winds (Fig. 3). Their lower height and wavelength indicate that mini-TARs consist of finer grain sizes than intra-crater TARs.

The ridges visible on the plain might represent a paleo bedform pattern. If so, features of this wavelength fits the TARs category [13] and their slightly different orientation than TARs inside craters and mini-TARs (Figs. 1c, 2 and 3) might point to different formative winds. However, the plain ridges are highly eroded and, at least in the studied area, do not preserve evidence of exposed cross-beds so formative winds have a 180° ambiguity. Alternatively, these features might represent periodic bedrock ridges (PBRs) [14, 15] which are erosional aeolian features seeded by megaripples [15]. This hypothesis is supported by the presence of fractures running from the bedrock to the ridges (Fig. 2). In both cases the action of the wind is the main trigger of their formation and, assuming a transverse trend to the main wind direction [14, 15], winds blowing from the NNE or the SSW can both explain their orientation. However, we cannot exclude a non-aeolian origin of the plain ridges that might just represent exposed layers of an underlying geological unit.

Because, this regularly spaced ridge pattern develops over the clay-bearing unit, it might represent a potential astrobiological target for the ESA Rosalind Franklin rover which can clarify the exact nature of these features. The meteorological package onboard of the ESA/ROSCOSMOS surface platform lander called Kazachok, which includes an anemometer and an im-

pect sensor, may shed light on the present-day wind regime in the landing site, providing an additional dataset to be compared with the bedforms observed from orbit and on the ground. The landing area shows the signs of climatic changes at different timescales. Part of these changes might be recorded by the aeolian bedforms covering the surface of the landing ellipse. The described aeolian features, can be directly accessible by the rover instruments providing precious hints on the climatic history of Mars.

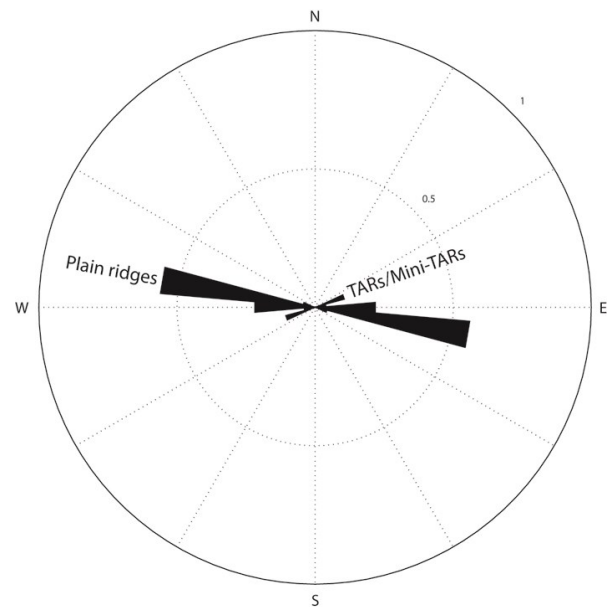


Fig. 3: Circular diagram showing the length-weighted distribution of the TARs and plain ridges in the study area. Note the different orientations.

References: [1] Vago et al. (2015). [2] Quantin et al. (2016, 47th LPSC, abstract # 2863. [3] Lakdawalla (2019), *Nature Astronomy* [4] Balme et al. (2017), *PSS*. [5] Pajola et al. (2017), *Icarus*. [6] Bhardwaj et al. (2019), *Remot.Sens*. [7] McEwen et al. (2007), *JGR*. [8] Malin et al. (2007), *JGR*. [9] Dickinson et al. (2018), 49th LPSC. [10] Golombek et al. (2010), *JGR*. [11] Fenton et al. (2013), *Treatise on Geomorphology* [12] Yizhaq et al. (2019), *EPSL*. [13] Hugenholtz et al. (2017), *Icarus*. [14] Montgomery et al. (2012), *JGR*. [15] Hugenholtz et al. (2015), *Icarus*.